

# Estimation of rockburst hazard basing on 3D stress field analysis

A. Tajduś, J. Flisiak & M. Cała  
University of Mining and Metallurgy, Kraków, Poland

**ABSTRACT:** This paper shows the possibilities of application of 3D numerical stress field analysis for estimation of rockburst hazard. The first part of the paper shows the proposition of rockburst hazard evaluation based on several indicators which are functions of stress tensor. The values of these indicators allow classification at an analysed region according to rockburst hazard. Two models of example mining situations with different roof geology were examined and the rockburst hazard was estimated. Finally, a real example of mining in rockburst hazard, utilising the introduced rockburst indicators, in one of the Polish underground coal mines was presented. The results from rockburst hazard estimation showed a good agreement with geophysical prognosis and registered rock mass seismicity.

## 1. INTRODUCTION

Rockbursts are one of the most dangerous hazards occurring during underground mining all over the world (Wong, 1992).

Many different methods are utilised for estimation of rockburst hazard. Generally these methods may be described as stochastic and deterministic. Stochastic methods are used to evaluate a probability of rockburst occurrence on the base of statistical analysis of registered seismic events and deterministic ones by investigation of factors which might cause rockburst.

Numerical analysis of stress tensor components has been applied for estimation of rockburst hazard in the past. Mainly flat models were investigated, (Zipf & Heasley, 1990; Faliang & Yile, 1991; Pan *et al.* 1991; Heasley, 1991; Pritchard & Hedley, 1993) but also in three dimensions (McCreary *et al.* 1993).

We would like to propose an original procedure of rockburst hazard evaluation based on 3D numerical analysis of the stress field.

## 2. DEFINITION OF ROCKBURST INDICATORS.

Assuming given components of stress tensor, four indicators for estimation of rockburst hazard may be calculated:

1. Coefficient of vertical stress concentration:

$$\alpha = \frac{\sigma_z(x, y, z)}{p_z} \quad (1)$$

where:

$\sigma_z(x, y, z)$  - vertical stresses in the elementary volume,

$p_z$  - initial, vertical stresses in the elementary volume.

2. Coefficient of energy concentration:

$$\beta = \frac{V_c}{V_c^i} \quad (2)$$

where:

$V_c$  - strain energy of the rock mass in the elementary volume,

$V_c^i$  - initial strain energy of the rock mass in the elementary volume (potential energy).

Energy  $V_c$  may be evaluated as:

$$V_c = V_o + V_p \quad (3)$$

where:

$V_o$  - strain energy of volume change,

$$V_o = \frac{1-2\nu}{6E} \left[ \sigma_x^2 + \sigma_y^2 + \sigma_z^2 + 2(\sigma_x\sigma_y + \sigma_y\sigma_z + \sigma_z\sigma_x) \right] \quad (4)$$

$V_p$  - strain energy of distortion,

$$V_p = \frac{1+\nu}{6E} \left[ (\sigma_x - \sigma_y)^2 + (\sigma_y - \sigma_z)^2 + (\sigma_z - \sigma_x)^2 + 6(\tau_{xy}^2 + \tau_{zx}^2 + \tau_{yz}^2) \right] \quad (5)$$

Initial elementary strain energy of the rock mass can be obtained as:

$$V_c^i = \frac{p_z^2(1-\nu-2\nu^2)}{2E(1-\nu)} \quad (6)$$

where:

$E, \nu$  - Young modulus and Poisson's coefficient in the elementary volume.

3. Ratio of effective stress to rock strength.

Assuming:  $\sigma_1 > \sigma_2 \geq \sigma_3$  ratio of effective stress to rock strength ( $W_b$ ) may be calculated utilising Burzyński's failure criterion as:

$$\circ \text{ if } \sigma_1 < R_r \text{ then } W_b^I = \frac{\sigma_o}{R_c} \quad (7)$$

where:  $R_c$  - uniaxial compressive strength,  
 $R_r$  - uniaxial tensile strength,  
 $R_t$  - shear strength,

$$\sigma_o = \frac{1}{2} \sqrt{\frac{3}{4} \left[ \frac{\sigma_i^2}{w_i^2} + 3\sigma_m^2 \left( \frac{6}{w_1} - \frac{4}{w_2} + \frac{3}{w_i^2} + 3 \right) \right]} + \frac{3}{2} \sigma_m \left( \frac{1}{w_1} - 1 \right) \quad (8)$$

$$\text{where: } w_1 = \frac{R_r}{R_c}, w_2 = \frac{R_t}{R_c} \quad (9)$$

$$\sigma_m = \frac{1}{3}(\sigma_1 + \sigma_2 + \sigma_3), \quad (10)$$

$$\sigma_i = \frac{1}{2}\sqrt{(\sigma_1 - \sigma_2)^2 + (\sigma_2 - \sigma_3)^2 + (\sigma_3 - \sigma_1)^2} \quad (11)$$

If shear strength of rock mass is unknown parabolic function of Burzyński's failure criterion may be adopted:

$$\sigma_o = \sqrt{\frac{\sigma_i^2}{w_l^2} + \left[ \frac{3}{2} \left( \frac{1}{w_l} - 1 \right) \sigma_m \right]^2} + \frac{3}{2} \left( \frac{1}{w_l} \right) \sigma_m. \quad (12)$$

$$\circ \text{ if } \sigma_1 \geq R_r \text{ then } W_b^{II} = \frac{\sigma_o}{R_r}. \quad (13)$$

In case when  $W_b^I > 1$ , shear failure of rock mass occurs and in case  $W_b^II > 1$ , tensile failure of rock mass occurs.

4. Energetic rockburst indicator - is calculated as the ratio of energy accumulated in the rock mass to the energy necessary for initiating rockburst. Energy balance of rockburst may be written as follows:

$$V_C + E_D = L_{ZN} + E_K + E_S + E_R \quad (14)$$

where:

$V_C$  - elastic energy accumulated in the broken rock mass during rockburst. This energy is a sum of initial stress field in the rock mass and stress field originated from mining,

$E_D$  - energy generated by the tremor in the rock mass,

$L_{ZN}$  - work used for breaking and crushing rock mass volume discharged to an opening,

$E_K$  - kinetic energy of crushed rock mass discharged to an opening,

$E_S$  - seismic energy developed during rockburst,

$E_R$  - dissipated energy.

The values of seismic and dissipated energy are very small compared to crushing work and kinetic energy. These two components can be neglected and the energy balance of rockburst may be formulated as:

$$V_C + E_D = L_{ZN} + E_K \quad (15)$$

Kinetic energy considerably influences the rockburst's results. It's minimal value can be estimated from the formula:

$$E_k^o = \frac{\rho_{sr} \cdot v_o^2}{2} \quad (16)$$

where:

$\rho_{sr}$  - average density of broken rock mass, assumed  $2.5 \cdot 10^3 \text{ kg/m}^3$ ,

$v_o$  - average velocity of broken rock mass ejected to an opening during rockburst, it may be estimated as  $v_o = 10 \text{ m/s}$  (Filcek, 1980).

After substituting the above data into equation (16) the initial kinetic energy of the rock mass during rockburst is equal to:

$$E_k^o = 1.25 \cdot 10^5 \frac{\text{J}}{\text{m}^3} \quad (17)$$

If the rock mass kinetic energy does not achieve initial value  $E_k^o$  rock mass is not capable to rockburst (probability of rockburst occurrence is very low). The multiple value of kinetic energy can be assumed as the energetic rockburst indicator -  $T_e$ :

$$T_e = \frac{E_k}{E_k^o} = \frac{V_C + E_D - L_{ZN}}{E_k^o} \quad (18)$$

If  $T_e < 1$  - rock mass is not capable of rockbursting (a rock fall may occur)

If  $T_e \bullet 1$  - occurrence of a rockburst is possible (probability of rockburst occurrence increases with the increase of  $T_e$  value). The energetic rockburst indicator is considered as the most important one. However, it must be noted that this indicator is calculated for the elementary volume and it should be calculated for all the volume of the failure zone.

After several years of application of presented above four rockburst hazard indicators and comparing its values with rock mass seismicity following rockburst hazard criteria may be formulated:

- when in given region the following conditions are fulfilled: concentration of vertical stresses ( $\alpha \geq 1.5$ ); elastic energy ( $\beta \geq 1.5$ ) rock mass is close to failure ( $W_b \approx 1$ ) and energetic rockburst indicator is low ( $T_e < 1$ ) then probability of rock tremors occurrence is very high. Energy of rock tremors depends on values of coefficient of energy concentration. The rock tremor may be estimated as:

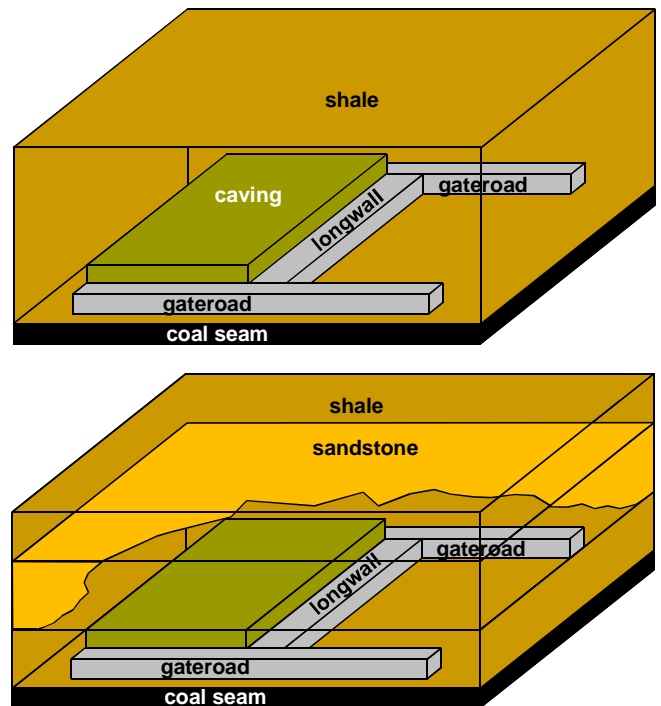


Fig.1. Image of 3D numerical models

$\beta \in (1.5, 3 > \Rightarrow$  low energy tremor,

$\beta \in (3, 5 > \Rightarrow$  medium-energy tremor,

$\beta \geq 5 \Rightarrow$  high-energy tremor.

- if the following conditions are fulfilled: considerable concentration of vertical stresses ( $\alpha \geq 2.0$ ); elastic energy ( $\beta \geq 3.0$ ) rock mass is close to failure ( $W_b \approx 1$ ) and energetic rockburst indicator is high ( $T_e \geq 1$ ) then there is a probability of rockburst occurrence.

Based on empirical evidence the probability of rockburst occurrence increases with coefficient of elastic energy concentration increase ( $\neq 5.0$ ) and energetic rockburst

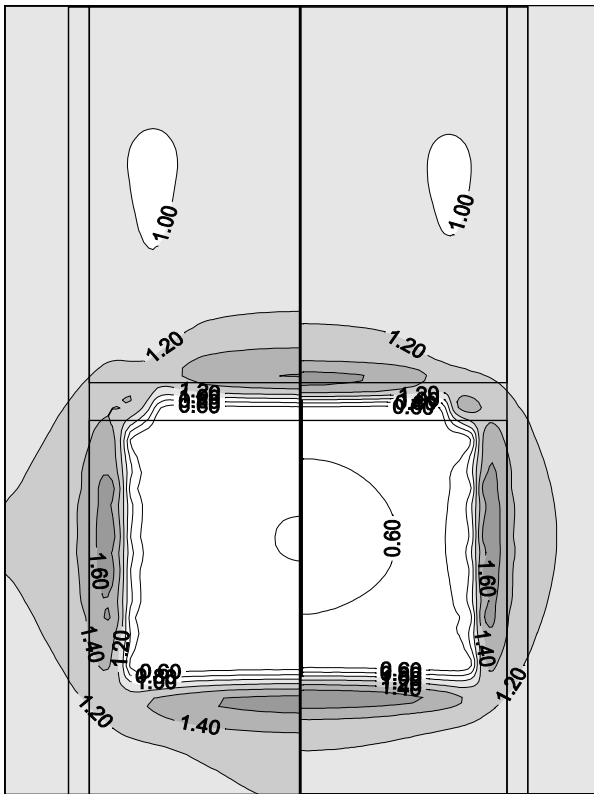


Fig.2. Distribution of  $\varphi$  for models I (left) and II(right)

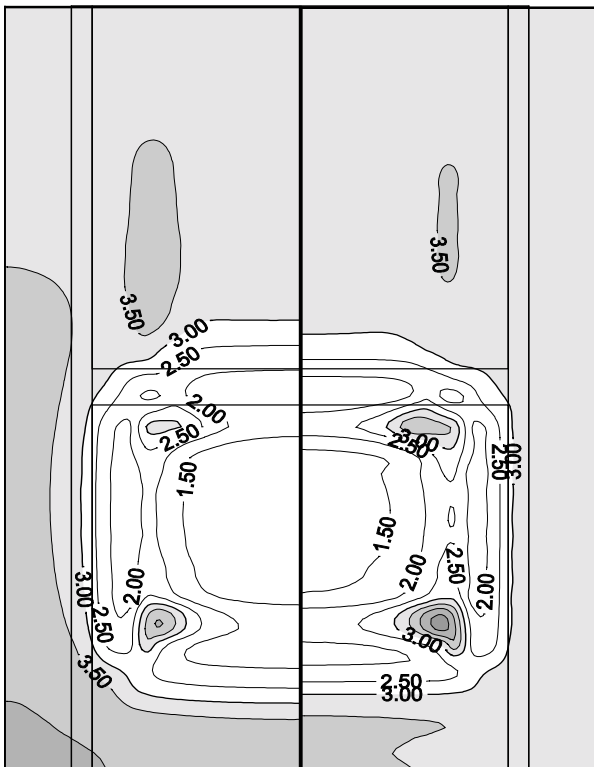


Fig.3. Distribution of  $\varphi$  for models I (left) and II(right)

indicator increase ( $T_e > 2.0$ ).

The presented criteria are the result of a calibration procedure performed for in last years. Several numerical models were calculated and results compared with seismic activity of the rock mass.

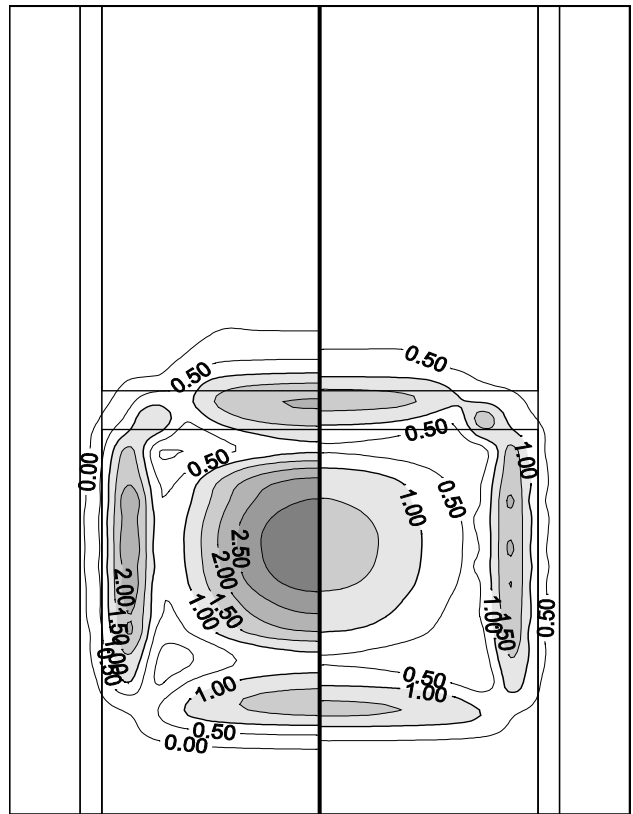


Fig.4. Distribution of Burzyński's effective stress for models I (left) and II(right)

### 3. APPLICATION OF ROCKBURST HAZARD INDICATORS FOR EXAMPLE MINING SITUATION.

To investigate the influence of rock mass geology on rockburst hazard 3D numerical calculations were performed. An example FEM 3D model was included vicinity of one longwall. In the first model the roof layers consisted of weak shale and in the second one, of hard sandstone just above coal seam (fig.1).

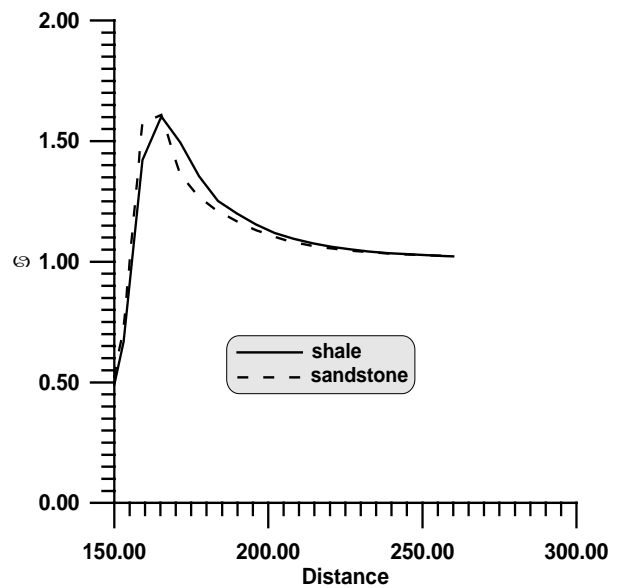


Fig.5. Diagram of  $\varphi$  coefficient for shale and sandstone roofs



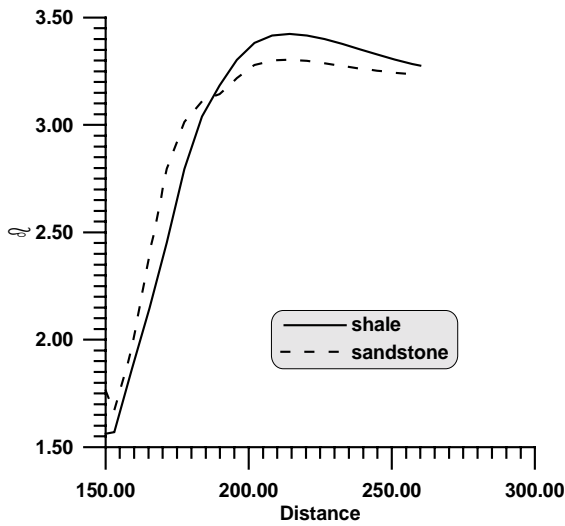


Fig.6. Diagram of  $\rho$  coefficient for shale and sandstone roofs

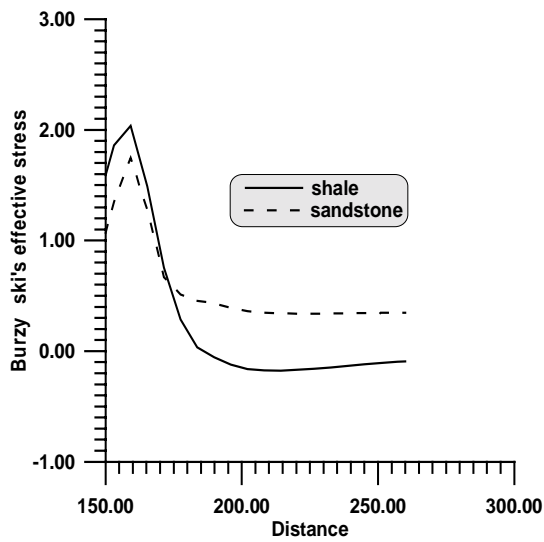


Fig.7. Diagram of Burzyński's effective stress for shale and sandstone roofs

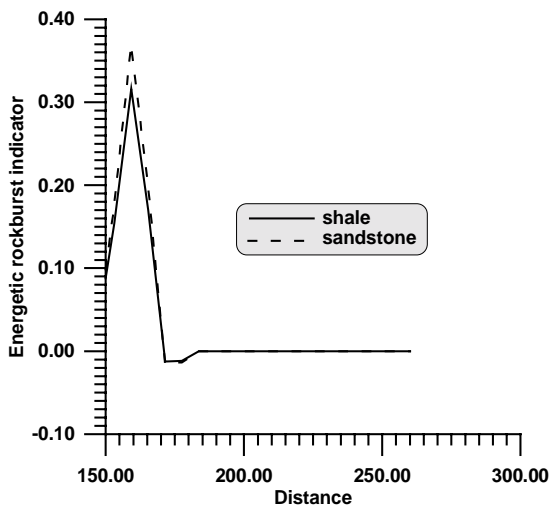


Fig.8. Diagram of energetic rockburst indicator for shale and sandstone roofs

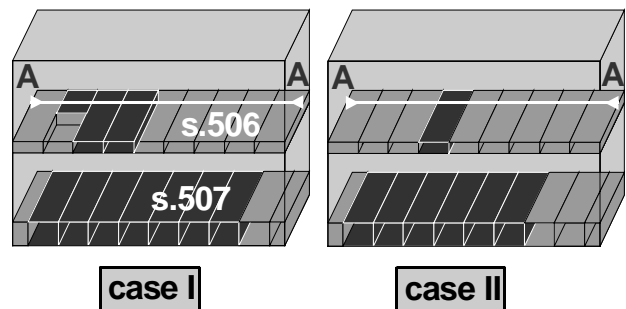
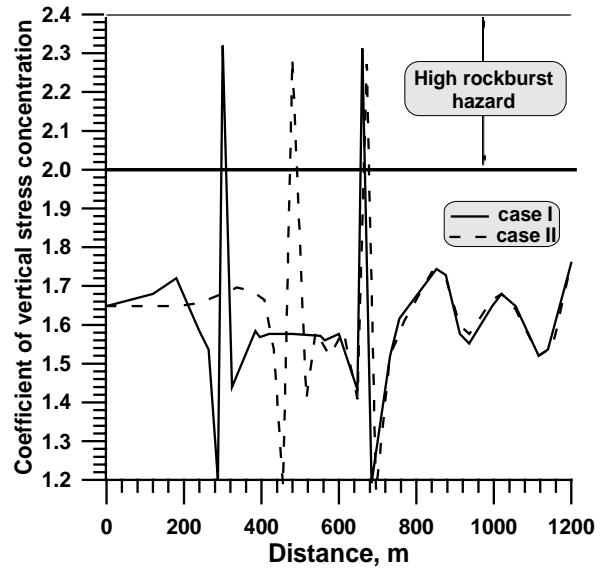


Fig.9. Distribution of  $\rho$  coefficient for analysed cases

For both models, the distribution of rockburst hazard indicators was determined after numerical calculation. Maps of rockburst hazard indicators distribution was done in the intersection distant 15m from coal seam roof (for model 1-shale stratum, for model 2 - sandstone stratum) Fig. 2, 3 and 4 show distributions of coefficient of vertical stress concentration; coefficient of energy concentration and ratio of effective stress to rock strength for model I (left side of the figure) and model II (right side of the figure) respectively.

The values of energetic rockburst indicator for both models did not exceeded 0.5 and the values of coefficient of vertical stress concentration did not exceeded 2.0. That's why we may suspect that rockburst hazard in analysed region is very low but several rock mass tremors maybe notified. The values of  $\rho$  and  $\tau$  coefficients are higher in case of sandstone roof. Ability of energy accumulation by hard rock stratum is a well known fact which influences rockburst hazard. That fact confirms suitability of proposed indicators for rockburst hazard estimation.

For better investigation of distribution of particular indicators intersection placed on symmetry axis of the model starting from longwall stope were also carried out (fig.5, 6, 7, 8). These intersections show that the values of coefficient of energy concentration and energetic rockburst indicator are higher in the vicinity of longwall for sandstone roof. Distribution of  $\tau$  coefficient is also very interesting. Considerable energy concentrations around longwall-gateroad junctions can be easily found for sandstone roof.

#### 4. APPLICATION OF 3D NUMERICAL CALCULATIONS FOR ROCKBURST HAZARD EVALUATION IN UNDERGROUND COAL MINE.

The presented system of rockburst hazard estimation was applied many times in Polish underground coal mines. For example longwall mining of two coal seams (506 and 507) was investigated (fig.9). The rock mass in the vicinity of both

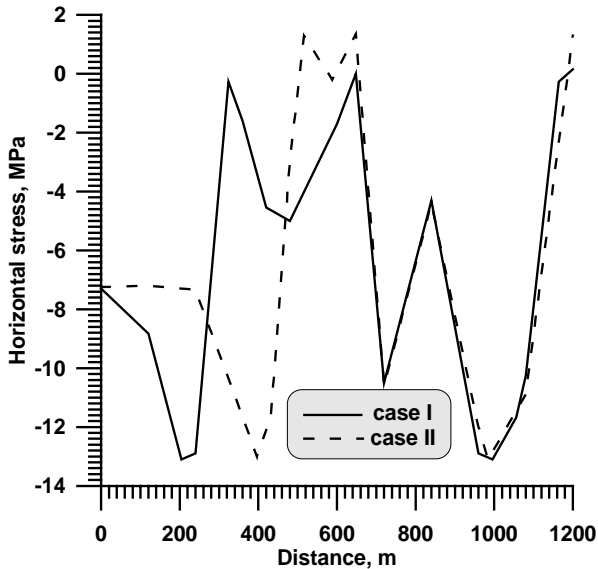


Fig.10. Distribution of vertical stress for case I and case II

coal seams consisted of hard layers capable for elastic energy accumulation due to mining.

Many rock tremors were noted during mining in seams no. 506 and 507. To estimate high rockburst hazard regions, 3D FEM numerical calculations for two different cases (fig.9) were performed (laminar plate model was utilised).

The aim of the numerical calculations was to determine how best to mine two last longwalls in seam 506 to minimise rockburst hazard. Mining situation in this case was very unfavourable because these two longwalls were closing seam 506.

Fig. 9 shows the distribution of coefficient of vertical stress concentration in the intersection A-A for both investigated cases. The range of extreme rockburst hazard is also noted on fig.9. The extreme rockburst hazard zone concentrates around gateroads and removes with the mining progress. Mining of following longwalls in seam no. 507 had no influence on rockburst hazard in seam 506.

By analysing the results it may also be determined that it's better to mine two longwalls together (with small advance) than mining each longwall separately. In case of single longwall excavation significant values of horizontal tension stresses occurs in hard roof layers. For two longwall excavation horizontal stresses are much smaller and mainly compressive (fig.10).

Summarising above remarks it may be stated that during mining in 506 seam, high seismic activity of the rock mass may be predicted, occurring of rockbursts is also possible. Conclusions presented above were confirmed by rockburst hazard prognosis utilising time-variable seismic risk analysis performed for that region (Lasocki *et al.* 1996).

#### 5. CONCLUSIONS

This paper presents an original method of estimating rockburst hazard in underground coal mines based on 3D numerical calculations of the stress field. Authors utilised FEM for this purpose. However, it's worth to notify that, depending on rock mass type and complexity of mining situation, other codes may also be used (BEM, FDM, DEM *etc.*). Higher accuracy of modelling any mining situation (excavation progress, initial stress state, discontinuities, faults, folds *etc.*) may give more realistic picture of rockburst hazard.

The main purpose of numerical calculation is estimation of stress tensor and later, evaluation of rockburst hazard indicators.

It has to be mentioned that rockburst hazard criteria presented below are valid only for geomechanical conditions of Polish underground coal mines. Application of proposed rockburst hazard estimation procedure for different conditions needs calibration. In the other words, one must perform several numerical experiments and later compare its results with seismic activity off the rock mass in analysed region.

#### 6. REFERENCES

- Faliang H. & Yile S. 1991. The relations between rockburst and the stresses around the stope in the Tian-Shen-Qiao tunnels. *Computer Methods and Advances in Geomechanics* (edited by Beer, Booker & Carter). A.A. Balkema. Rotterdam, pp. 1333-1338.
- Filcek H. 1980. Geomechanical criteria of rockburst hazard. *Zeszyty Naukowe AGH, Górnictwo no.4, Kraków*, (in polish).
- Heasley K.A. 1991. An examination of energy calculations applied to coal bump prediction. *Proc. of 32<sup>nd</sup> U.S. Symposium on Rock Mechanics*. (edited by J.C. Roegiers). A.A. Balkema. Rotterdam, pp. 1481-490.
- Lasocki S., Matuszyk J. & Szybiński M. 1996. Estimating of seismic hazard utilising seismic risk method. *Unpublished materials*, Kraków (in polish).
- McCreary R.G., Grant D. & Falamagne V. 1993. Source mechanisms, three-dimensional boundary element modelling and underground observation at Ansil Mine. *Proceedings of Int. Conf. Rockburst and Seismicity in Mines* (edited by Young), A.A. Balkema, pp. 111-116.
- Pan Y., Liu C. & Zhang M. 1991. The numerical simulation of time effect of coal burst. *Computer Methods and Advances in Geomechanics* (edited by Beer, Booker & Carter). A.A. Balkema. Rotterdam, pp.1375-1379.
- Pritchard C.J. & Hedley D.G.F. 1993. Progressive pillar failure and rockbursting at Denison Mine. *Proceedings of Int. Conf. Rockburst and Seismicity in Mines* (edited by Young), A.A. Balkema, pp. 111-116.
- Wong I.W. 1992. Recent developments in rockburst and mine seismicity research. *Proceedings of 33<sup>rd</sup> U.S. Symposium on Rock Mechanics*. (ed. by Tillerson & Wawersik). A.A.Balkema. Rotterdam, pp. 1103-1112.
- Zipf R.K. & Heasley K.A. 1990. Decreasing coal bump risk through optimal cut sequencing with a non-linear boundary element program. *Proc. of 31<sup>st</sup> U.S. Symposium on Rock Mechanics* (edited by W.A. Hustrulid & G.A. Johnson), A. A. Balkema. Rotterdam, pp. 77-84.